Since January 2020 Elsevier has created a COVID-19 resource centre with free information in English and Mandarin on the novel coronavirus COVID-19. The COVID-19 resource centre is hosted on Elsevier Connect, the company's public news and information website.

Electrochemistry Communications 120 (2020) 106833

Contents lists available at ScienceDirect

Electrochemistry Communications

journal homepage: www.elsevier.com/locate/elecom

Electrochemical removal of anodic aluminium oxide templates for the production of phase-pure cuprous oxide nanorods for antimicrobial surfaces

Kevin P. Musselman[a,b,*], Louis-Vincent Delumeau[a,b,*], Roy Araujo[e], Haiyan Wang[c,*], Judith MacManus-Driscoll[d,*]

[a] Department of Mechanical and Mechatronics Engineering, University of Waterloo, 200 University Ave. West, Waterloo, Canada
[b] Waterloo Institute for Nanotechnology, 200 University Ave. West, Waterloo, Canada
[c] School of Electrical and Computer Engineering, Purdue University, West Lafayette, IN 46907, USA
[d] Department of Materials Science & Metallurgy, University of Cambridge, 27 Charles Babbage Road, Cambridge CB3 0FS, United Kingdom
[e] Department of Electrical & Computer Engineering, Texas A&M University, 400 Bizzell St., College Station, TX 77843, USA

ARTICLE INFO

Keywords:
Anodic aluminum oxide
Antimicrobial surfaces
Nanorod array
Cuprous oxide
Electrochemical template removal

ABSTRACT

Antimicrobial surfaces are ones that incapacitate or kill pathogens landing on them, which could allow for self-sanitising surfaces for hospitals or implants, ensuring healthier stays and procedures. Cuprous compounds such as Cu_2O are especially effective at incapacitating both viruses and bacteria, and nanorod arrays have been shown to prevent the adhesion of pathogens and mechanically deform bacteria to the point that their cell walls rupture. A Cu_2O nanorod array should therefore allow for the exploitation of both of these effects. In the present work, an electrochemical method is introduced, where Cu_2O nanorods formed in a substrate-supported anodic aluminium oxide (AAO) template are held at a stable electrochemical potential throughout the removal of the AAO template. This avoids the partial reduction of the nanorods from Cu_2O to Cu that was observed during chemical removal of the template, which was attributed to the presence of residual aluminium from the template fabrication process that reacts with the etchant and lowers the electrochemical potential of the nanorods to a value that favours reduction. Using the electrochemical removal method, the reliable production of phase-pure, free-standing, crystalline Cu_2O nanorod arrays on ITO/glass substrates is demonstrated. This simple method is compatible with nanorod arrays of any size.

1. Introduction

Anodic aluminium oxide (AAO) templates have proven to be a useful tool for producing arrays of nanorods, nanowires, and nanotubes (both semiconducting and metallic), for applications in sensing, energy generation and storage, and catalysis [1–3]. These templates have been produced on aluminium (Al) foils, as well as different substrates, including silicon and indium-tin-oxide (ITO)/glass [3–9]. With the rise in antibiotic resistance in bacteria and the recent difficulty in tackling the COVID-19 viral pandemic, there is an urgent need for enhanced antimicrobial surfaces, and template-created arrays are a promising architecture for such surfaces.

Nanorod or nanowire arrays can impart antimicrobial properties to a surface by preventing the adhesion of pathogens and/or incapacitating them once they reach it [10,11]. Poor adhesion follows from the fact that nanotextured surfaces are hydrophobic, due to the air they retain between the nano-features, which minimises contact area between pathogens and the surface [11]. Incapacitation of adhered pathogens may follow from physical and/or chemical effects. Arrays of nearly parallel nanorods have been developed as bactericidal “beds of nails”, inspired from the bactericidal nanorod-rich surfaces of certain insect wings [10,12–14]. Evidence has indicated that the SARS-CoV-2 virus is less viable on copper (Cu) surfaces than on other common surfaces [15], and more specifically, cuprous compounds are among the most effective materials known to incapacitate pathogens, including SARS-CoV-2 [16–18]. In a study using human coronavirus 229E on Cu/Zn brass samples for example, it was found that Cu(I) may play a more significant role in virus incapacitation than Cu(II) in the longer term [19]. In another study, cuprous oxide (Cu_2O) powders reduced the infectious activity of bacteriophage T4 and Qβ viruses by 4 and 5 orders of magnitude in 30 min and the infectious activity of gram-negative and gram-positive bacteria by 3 orders of magnitude in 1 h. These

* Corresponding authors.
E-mail addresses: kevin.musselman@uwaterloo.ca (K.P. Musselman), ldelumeau@uwaterloo.ca (L.-V. Delumeau), hwang00@purdue.edu (H. Wang), jld35@cam.ac.uk (J. MacManus-Driscoll).

https://doi.org/10.1016/j.elecom.2020.106833
Received 29 August 2020; Received in revised form 13 September 2020; Accepted 14 September 2020
Available online 18 September 2020

reductions were significantly larger than for CuO or silver powders, and it was concluded that the mode of action to degrade pathogen biomolecules must be direct contact with cuprous compound surfaces [16].

Thus, the ability to control the chemical composition of antimicrobial surfaces is critical. In the case of nanorod fabrication with AAO templates, the templates are typically removed by chemically etching the AAO in a basic solution. However, little consideration has been given to the influence of etching on the embedded materials. In this work we examine the chemical stability of Cu_2O nanorods, a promising antimicrobial surface due to the combined effect of Cu_2O and of nano-features, during the chemical removal of a surrounding AAO template.

2. Materials and methods

2.1. Nanorod fabrication

Cu_2O nanorod arrays were fabricated using AAO templates on ITO/glass by a procedure reported previously [3], as illustrated in Fig. 1. Briefly, Al films approximately 500 nm thick were deposited onto ITO/glass substrates (Praezisions Glas & Optik) by DC magnetron sputtering with thin titanium (Ti) and tungsten (W) adhesion and barrier layers between the ITO and Al. The Al films were then anodised in 0.3 M oxalic acid at 40 V to produce AAO templates approximately 800 nm thick. The edges of the samples were masked with Crystal bond adhesive to prevent delamination from the edges during anodisation. After anodisation, the AAO templates were soaked in 5 wt% phosphoric acid to widen the pores slightly and remove the oxide layer from the base of the pores, exposing the underlying conductive substrate. Cu_2O was then electrochemically deposited into the AAO pores to produce arrays of Cu_2O nanorods with approximate dimensions of 60 nm in diameter and 300 nm in length. All details for the nanorod fabrication can be found in a previous report [3]. Cu_2O films were also produced using identical electrochemical deposition conditions by using bare ITO/glass substrates as the working electrode.

2.2. Chemical removal of AAO templates

The AAO templates were chemically removed to leave free-standing nanorod arrays by soaking in an aqueous 0.1 M NaOH solution for 30 min, as illustrated in Fig. 1. After template removal, the nanorod samples were rinsed in purified water to remove any remaining NaOH and dried with a light flow of nitrogen. To monitor the electrochemical potential of a nanorod array during the chemical template removal process, an insulated Cu wire was attached to the underlying ITO substrate with silver (Ag) paste and masked with Kapton polyimide tape. The potential of the sample was measured using a Keithley 2400 Sourcemeter, relative to an Ag/AgCl (in saturated KCl) reference electrode, which was also inserted into the etching solution.

2.3. Electrochemical removal of AAO templates

For the electrochemical template removal procedure, an insulated Cu wire was attached with Ag paste to the underlying ITO substrate of the sample to be etched, and masked with Kapton polyimide tape. The sample was then attached to a Princeton Applied Research Model 363 Potentiostat/Galvanostat in a standard three-electrode configuration with a reference electrode like the one described in Section 2.2 and a 6.25 cm^2 platinum counter electrode, as illustrated in Fig. 1. The electrodes (including the sample to be etched) were immersed in 0.1 M aqueous NaOH at room temperature, at which point the potentiostat was turned on immediately. After template removal, the nanorod samples were rinsed in purified water to remove any remaining NaOH and dried with a light flow of nitrogen.

2.4. Materials characterisation

Scanning electron microscopy (SEM) was performed with a a LEO VP1530 field emission SEM. Phase identification was performed using a Bruker D8 theta/theta X-ray diffraction (XRD) system with Cu Kα radiation (λ = 0.15418 nm) and a LynxEye position-sensitive detector. The transmission electron microscopy (TEM) cross-sectional specimen

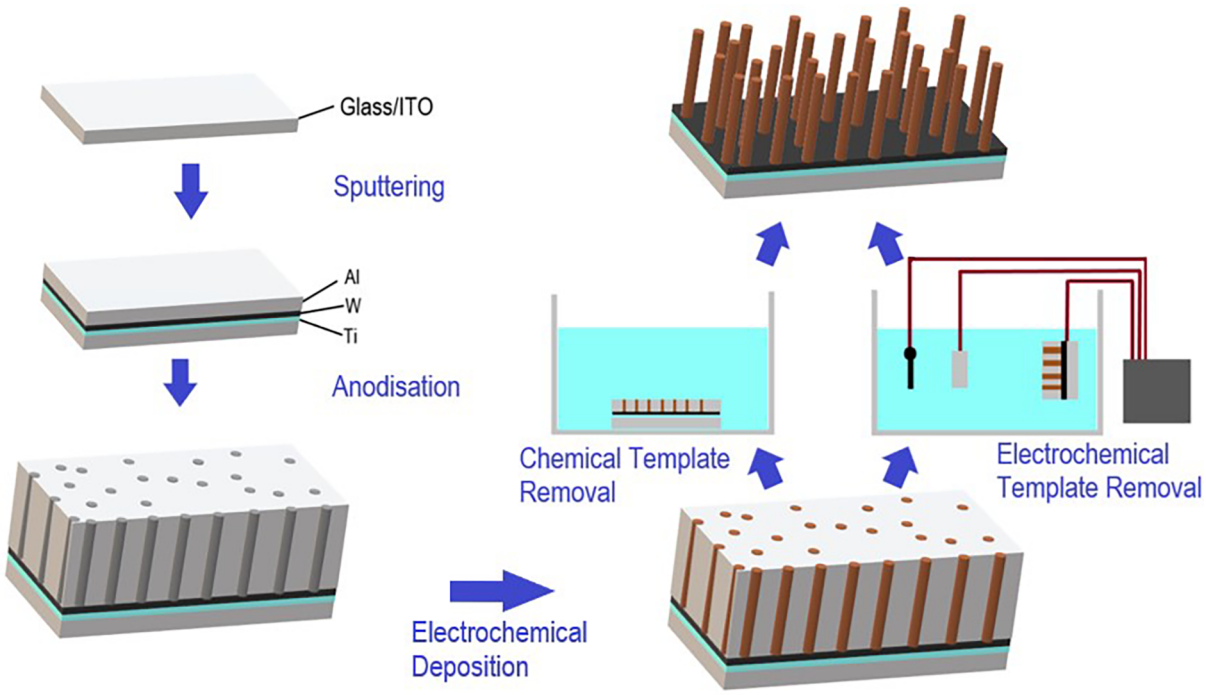

Fig. 1. Overview of Cu_2O nanorod array fabrication process.

was prepared by conventional mechanical thinning, grinding, polishing, and a final ion polishing step. The TEM images were taken using a FEI Tecnai F20 electron microscope. Cyclic voltammetry of Cu_2O films was performed using the same potentiostat/galvanostat and three-electrode cell noted in Section 2.3, together with custom-made Labview software.

3. Results and discussion

3.1. Instability of Cu_2O nanorod arrays during chemical removal of AAO

Top-view SEM images of the fabricated AAO templates are shown in Fig. 2a–b. The pore diameters are observed to range in size from approximately 30 to 60 nm. Fig. 2c shows a top-view SEM image of a nanorod array produced by pore-widening the AAO template for 30 min in the 5 wt% phosphoric acid, followed by electrochemical deposition of Cu_2O and chemical removal of the AAO template. Image analysis

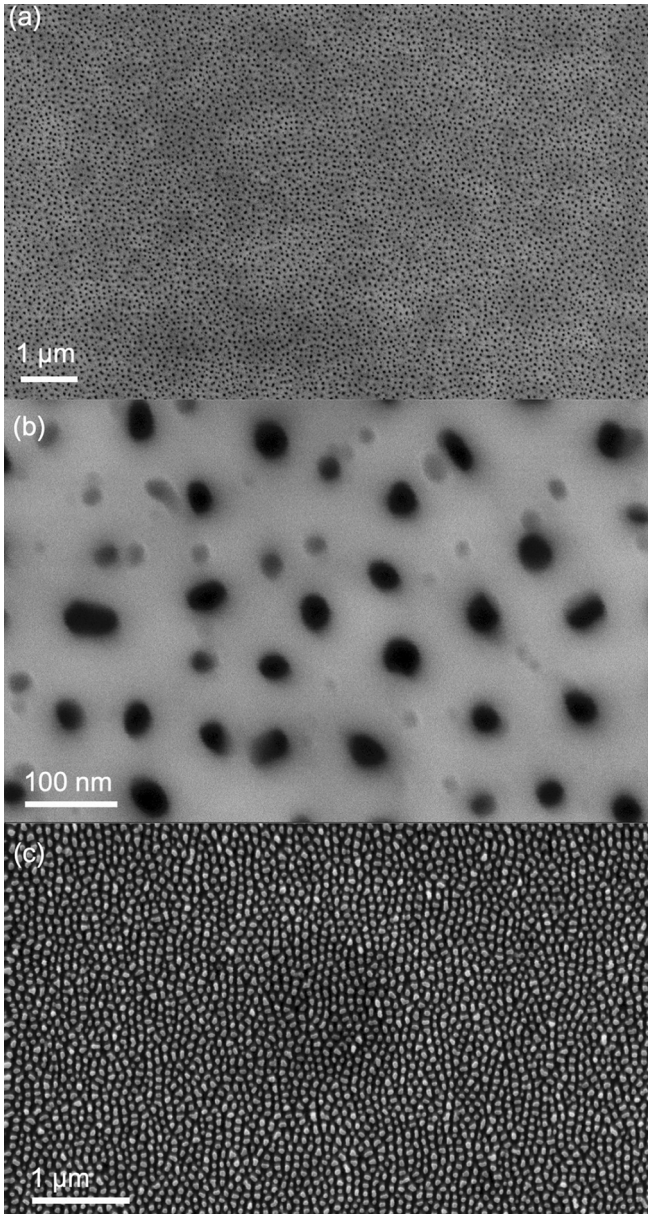

Fig. 2. (a–b) SEM images of AAO template on ITO/glass substrate formed by anodisation at room temperature in 0.3 M oxalic acid at 40 V. (c) Nanorod array formed by electrochemical deposition of Cu_2O into the AAO, followed by chemical removal of the AAO.

indicated an average nanorod diameter of 53 ± 8 nm. The bactericidal efficiency has been reported to depend on the dimensions of the nanostructures, and the nanorod arrays produced here fall well within the recommended dimensions for bactericidal nanostructures [12,14].

The XRD data for an AAO template on ITO/glass, containing an array of Cu_2O nanorods approximately 275 nm long is shown in Fig. 3a. The XRD data indicates that the nanorods are phase pure. Other than signals associated with the ITO substrate and AAO template, the only peaks present in the as-deposited sample correspond to Cu_2O. Moreover, the intensity and sharpness of the peaks indicate a good degree of crystallinity of the Cu_2O phase grown by the electrodeposition technique. Fig. 3b shows the XRD data for a similar nanorod array after template removal by chemical etching. The intensity of all Cu_2O peaks was reduced by the chemical template removal procedure and a Cu peak appeared. Removal of the AAO template by chemical etching was seen to result in discolouration of the nanorods from bright yellow to brown, as shown in Fig. 3d, consistent with partial reduction of the Cu_2O nanorods to elemental copper.

The Cu peak in Fig. 3b is broad, indicating small crystallites of Cu are formed during the reduction process. From the breadth of the peak, the Cu crystallite size was estimated to be approximately 20 nm using the Scherrer equation. This was confirmed by TEM imaging. Fig. 4a shows a cross-sectional TEM image of 300 nm-tall nanorods for which discolouration was observed during template removal. The nanorods are seen to be composed of many small grains. Fig. 4b–c show the phase-pure Cu_2O nanorods removed from AAO templates by the electrochemical technique. Very clear nanorods structures are seen with an average rod length of 200 nm and an average diameter of 50 nm.

The electrochemical potential of a Cu_2O nanorod array during the chemical template removal process was measured and is shown in Fig. 5a. The potential of the nanorod array was observed to drop to a value significantly lower than −0.5 V within the first few minutes of etching, before returning to a more positive potential, after approximately 16 min. The lower half of the inset in Fig. 5 displays pictures taken of the sample surface during chemical template removal, at intervals of 1 min. Significant discolouration of the Cu_2O nanorods is seen, particularly after 11 min, when the potential dropped to a value less than −1.1 V.

Chemical removal of AAO is performed at room temperature in a simple aqueous NaOH solution, such that the etching conditions are well described by the electrochemical stability diagram of Pourbaix [20], reproduced in Fig. 6. For the copper system in aqueous solutions at 25 °C and a pH of 13, the reduction of Cu_2O to Cu is favoured at potentials of approximately −0.5 V (versus Ag/AgCl in KCl(sat)) or lower [20]. This is consistent with the reduction to metallic copper observed in the inset of Fig. 5a, particularly when the electrochemical potential dropped below −1.1 V.

We attribute the negative potential observed during the initial stage of the chemical template removal to the presence of residual aluminium from the AAO template fabrication process. Areas of un-anodised Al are present on the samples due to (1) the masking of the edges to prevent delamination during anodisation (as noted in Section 2.1), and (2) the masking of an area of the sample for electrical connection during anodisation and electrochemical deposition. This Al is visible in Fig. 3d. Residual Al may also exist at the base of the substrate-supported AAO template, due to incomplete anodisation of the aluminium [1]. Aluminium is expected to oxidise and dissolve in basic solutions according to the following reactions [20]:

$$2Al + 3H_2O \rightarrow Al_2O_3 + 6H^+ + 6e^-$$

$$Al + 2H_2O \rightarrow AlO_2^- + 4H^+ + 3e^-$$

These reactions result in the production of free electrons and hence would lower the electrochemical potential of the sample. The potential variations observed over the first 12 min in Fig. 5a likely arise from changes in the amount of residual Al exposed to the etching solution as

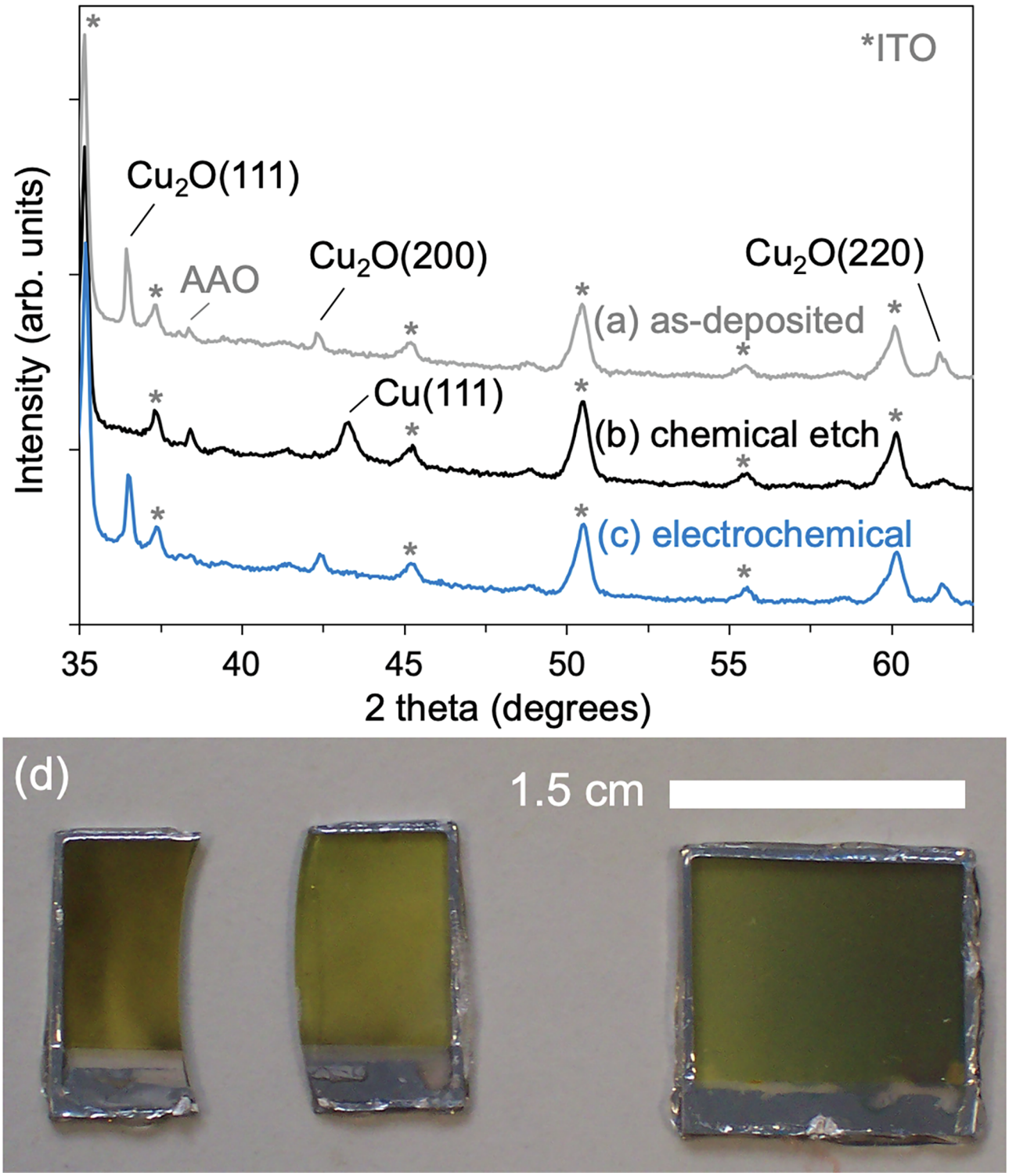

Fig. 3. XRD data of (a) as-deposited Cu_2O nanorods in AAO templates, (b) Cu_2O nanorods after chemical removal of the AAO template, and (c) Cu_2O nanorods after electrochemical removal of the template. The intensity of the Cu_2O peaks is reduced and an elemental Cu peak appears after chemical etching whereas the Cu_2O peaks are unchanged by the electrochemical etching. (d) Picture of Cu_2O nanorod arrays after chemical removal of AAO template. Significant discolouration was observed, whether the samples were etched whole or in pieces.

the AAO template is removed. After 15 min little Al remained, such that fewer electrons were available for the reduction of the Cu_2O, resulting in an increase in the sample potential (Fig. 5a). When central portions of the Cu_2O nanorod samples were selected to limit the amount of residual Al present, the degree of discolouration observed during chemical removal of the AAO template was reduced significantly. These observations strongly suggest that the apparent reduction of Cu_2O nanorods during chemical removal of the AAO template is due to the

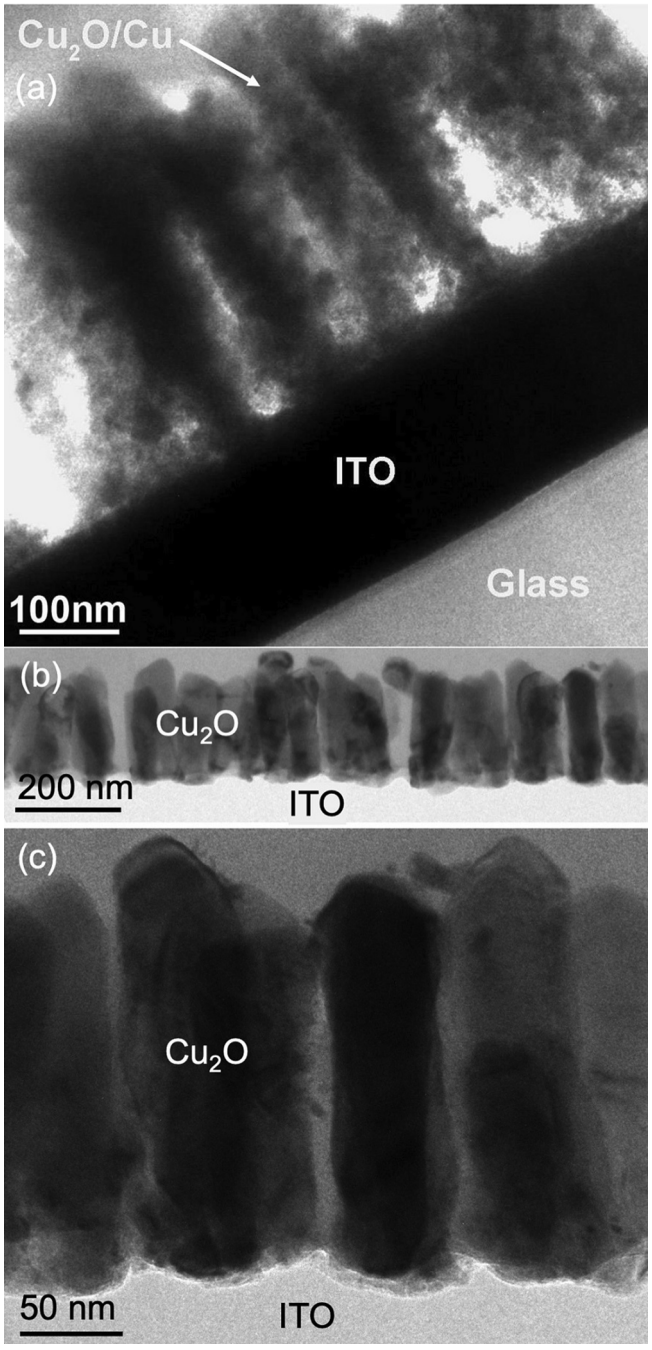

Fig. 4. Cross-sectional TEM images of (a) partially reduced Cu_2O/Cu nanorods formed from Cu_2O nanorods during chemical removal of AAO templates, and (b–c) phase-pure Cu_2O nanorods removed from AAO templates by the electrochemical technique.

presence of residual aluminium. To confirm this, the Cu_2O thin films synthesised using identical electrochemical deposition conditions on identical ITO/glass substrates were soaked in the etching solution in a similar manner. These samples contain no Al and correspondingly no reduction of the Cu_2O was observed visibly or by XRD analysis.

3.2. Electrochemical removal of AAO templates

It is crucial to be able to remove AAO template without altering the properties of the nanostructures contained therein, particularly for surface-sensitive applications such as antimicrobial coatings. This necessitates the ability to maintain the electrochemical potential of the

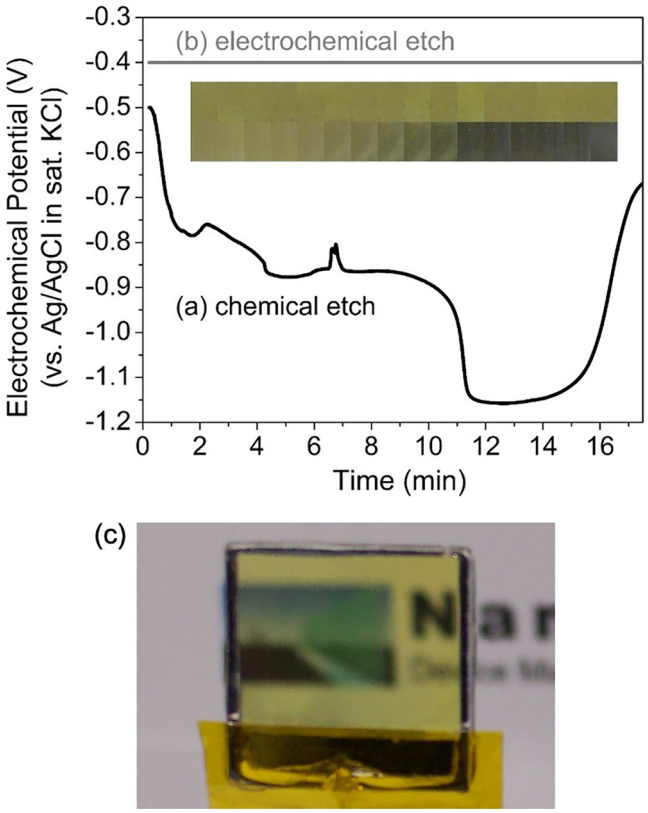

Fig. 5. Electrochemical potential measurements of Cu_2O nanorod arrays during (a) chemical removal and (b) electrochemical removal of the surrounding AAO templates. Inset: pictures of the nanorod sample surfaces at 1 min intervals for the chemical (lower) and electrochemical (upper) template removal methods. (c) Picture of Cu_2O nanorod array after electrochemical removal of AAO template.

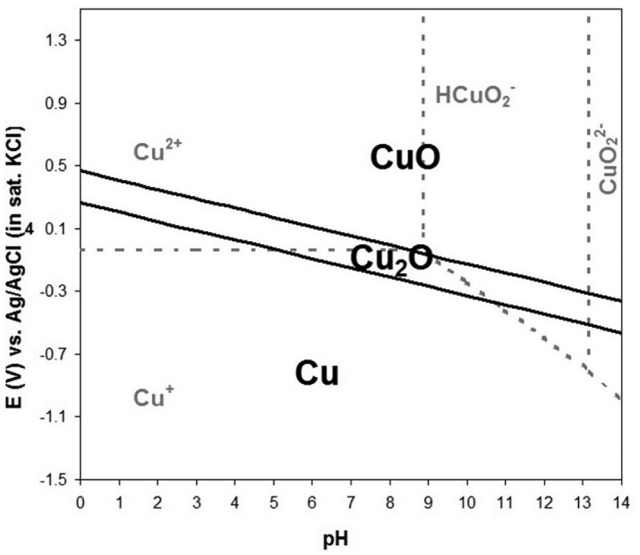

Fig. 6. Electrochemical stability Pourbaix diagram for the aqueous copper–-copper oxide system at room temperature. It can be used to determine the electrochemical stability of Cu_2O in 0.1 M NaOH etching solution.

nanorod array at a level within the stability region throughout the template removal process. Using the setup detailed in Section 2.3, the electrochemical potential of the ITO substrate and Cu_2O nanorod array was held at a fixed value of −0.4 V, which corresponds to the middle of the Cu_2O stability region at a pH of 13 (Fig. 6). Fig. 5b shows the

constant potential maintained throughout the electrochemical template removal, and the upper portion of the inset in Fig. 5 displays pictures of a Cu_2O nanorod sample at 1 min intervals during the electrochemical template removal. In contrast to the chemical template removal (lower portion of inset), no change in colour was observed. Nanorod arrays were maintained in these electrochemical conditions for over 3 h with no visible change in colour. Fig. 5c shows a Cu_2O nanorod array produced via this electrochemical template removal approach. It is seen in Fig. 6 that the Cu_2O stability region is equally narrow across the entire pH range, so the electrochemical template removal is expected to be advantageous regardless of the pH of the etching solution used, provided an appropriate potential is selected for the nanorod array to be maintained at.

The nanorods subjected to this prolonged 3-hour template removal process were examined by TEM and XRD. The XRD data of the electrochemically treated nanorods is shown in Fig. 3c and was identical to that of the as-deposited nanorods (Fig. 3a), except for the absence of an AAO-related peak, indicating that phase-pure Cu_2O remained. TEM images of the nanorods removed from the AAO using the electrochemical method are shown in Fig. 4b–c. Compared to the nanorods produced by chemical removal of the AAO in Fig. 4a, the electrochemically-removed nanorods display large crystalline grains with dimensions similar to the nanorods themselves. This is consistent with the sharper Cu_2O XRD peaks from Fig. 3a and c.

4. Conclusions

The reliable production of pure, crystalline nanorod arrays on supporting substrates via the removal of AAO is critical for the realisation of many of the proposed applications of these nanostructures. To prevent reduction of nanorods in AAO templates upon template dissolution, Cu_2O nanorods were studied. An easy-to-implement electrochemical template removal method was employed, in which the Cu_2O nanorods were held at a stable electrochemical potential throughout the AAO etching process, guaranteeing Cu_2O nanorods as a final product. It was found that the presence of residual aluminium from the AAO template leads to a negative electrochemical potential on the sample and partial reduction of the Cu_2O to metallic Cu during chemical template removal. By introducing this simple electrochemical procedure to remove the ITO-supported AAO, we demonstrate the ability to produce phase-pure Cu_2O nanorod arrays. To our knowledge, there has been no previous report of a similar electrochemical technique for the removal of AAO templates. This technique would be similarly useful for other materials with limited electrochemical stability, such as iron, zinc, chromium, and manganese oxides. Moreover, it is compatible with conductive substrates of any size, and could have applications in mass production of nanostructures. Notably, these phase-pure Cu_2O nanorod arrays are promising as antimicrobial surfaces that may prevent the adhesion of pathogens and/or incapacitate them through morphological mechanisms and the material effects of Cu_2O. This could be very useful in applications such as antimicrobial surfaces in hospitals. The synthesis method developed in this work will facilitate future investigation of the antimicrobial behavior of these and other types of nanorod arrays.

Authors contribution

K.P. Musselman performed all experiments except for the TEM. R. Araujo and H. Wang performed the TEM. K.P. Musselman and J. MacManus-Driscoll analysed the results. K.P. Musselman and L. Delumeau wrote the manuscript. J. MacManus-Driscoll and H. Wang reviewed the manuscript.

CRediT authorship contribution statement

Kevin P. Musselman: Conceptualization, Methodology, Validation, Investigation, Writing - original draft, Writing - review & editing, Visualization, Funding acquisition. **Louis-Vincent Delumeau:** Conceptualization, Investigation, Writing - original draft, Writing - review & editing, Visualization. **Roy Araujo:** Visualization. **Haiyan Wang:** Writing - review & editing, Visualization. **Judith MacManus-Driscoll:** Conceptualization, Methodology, Resources, Writing - review & editing, Supervision, Project administration, Funding acquisition.

Declaration of Competing Interest

The authors declare that they have no known competing financial interests or personal relationships that could have appeared to influence the work reported in this paper.

Acknowledgements

Funding: This work was supported by Girton College (University of Cambridge, U.K.); the Ontario Ministry of Colleges and Universities [grant number ER18-14-263]; and the U.S. National Science Foundation [grant numbers DMR-1565822 and DMR-2016453].

References

[1] W. Lee, S.-J. Park, Porous anodic aluminum oxide: anodization and templated synthesis of functional nanostructures, Chem. Rev. 114 (15) (2014) 7487–7556.
[2] X. Ren, T. Gershon, D.C. Iza, D. Muñoz-Rojas, K. Musselman, J.L. MacManus-Driscoll, The selective fabrication of large-area highly ordered TiO 2 nanorod and nanotube arrays on conductive transparent substrates via sol–gel electrophoresis, Nanotechnology 20 (36) (2009) 365604, https://doi.org/10.1088/0957-4484/20/36/365604.
[3] K.P. Musselman, G.J. Mulholland, A.P. Robinson, L. Schmidt-Mende, J.L. MacManus-Driscoll, Low-temperature synthesis of large-area, free-standing nanorod arrays on ITO/glass and other conducting substrates, Adv. Mater. 20 (23) (2008) 4470–4475.
[4] T.R.B. Foong, A. Sellinger, X. Hu, Origin of the bottlenecks in preparing anodized aluminum oxide (AAO) templates on ITO glass, ACS Nano 2 (11) (2008) 2250–2256.
[5] J. Byun, J.I. Lee, S. Kwon, G. Jeon, J.K. Kim, Highly ordered nanoporous alumina on conducting substrates with adhesion enhanced by surface modification: universal templates for ultrahigh-density arrays of nanorods, Adv. Mater. 22 (18) (2010) 2028–2032.
[6] A.F. Feil, P. Migowski, J. Dupont, L. Amaral, S.R. Teixeira, Nanoporous aluminum oxide thin films on si substrate: structural changes as a function of interfacial stress, J. Phys. Chem. C 115 (15) (2011) 7621–7627.
[7] T.R.B. Foong, Y.N. Liang, X. Hu, Anodic aluminum oxide (AAO) templates on transparent conducting glass (TCO) coated glass: new prospects for a mature nanofabrication tool, Nanosci. Nanotechnol. Lett. 4 (5) (2012) 494–504.
[8] C. Hong, R. Pan, W. Fang, 26.3: development of nanoporous anodic aluminum oxide (np-AAO) thin template on PET/Ti flexible substrate for flexible liquid cristal display (flexible-LCD) application, SID Int. Symp. Dig. Tec. 43 (2012) 348–351, https://doi.org/10.1002/j.2168-0159.2012.tb05787.x.
[9] B. Wang, G. Xu, P. Cui, Preparation of large-area porous anodic alumina on insulating substrates, Mater. Lett. 93 (2013) 36–38.
[10] S. Rigo, C. Cai, G. Gunkel-Grabole, L. Maurizi, X. Zhang, J. Xu, C.G. Palivan, Nanoscience-based strategies to engineer antimicrobial surfaces, Adv. Sci. 5 (5) (2018) 1700892, https://doi.org/10.1002/advs.v5.510.1002/advs.201700892.
[11] R.Y. Siddiquie, A. Agrawal, S.S. Joshi, Surface alterations to impart antiviral properties to combat COVID-19 transmission, Trans. Indian Natl. Acad. Eng. 5 (2) (2020) 343–347.
[12] A. Jaggessar, H. Shahali, A. Mathew, P.K.D.V. Yarlagadda, Bio-mimicking nano and micro-structured surface fabrication for antibacterial properties in medical implants, J. Nanobiotechnol. 15 (1) (2017), https://doi.org/10.1186/s12951-017-0306-1.
[13] E. Jeong, C.U. Kim, J. Byun, J. Lee, H.-E. Kim, E.-J. Kim, K.J. Choi, S.W. Hong, Quantitative evaluation of the antibacterial factors of ZnO nanorod arrays under dark conditions: physical and chemical effects on Escherichia coli inactivation, Sci. Total Environ. 712 (2020) 136574, https://doi.org/10.1016/j.scitotenv.2020.136574.
[14] A. Tripathy, P. Sen, B.o. Su, W.H. Briscoe, Natural and bioinspired nanostructured bactericidal surfaces, Adv. Colloid Interface Sci. 248 (2017) 85–104.
[15] N. van Doremalen, T. Bushmaker, D.H. Morris, M.G. Holbrook, A. Gamble, B.N. Williamson, A. Tamin, J.L. Harcourt, N.J. Thornburg, S.I. Gerber, J.O. Lloyd-Smith, E. de Wit, V.J. Munster, Aerosol and surface stability of SARS-CoV-2 as

compared with SARS-CoV-1, N Engl J Med 382 (16) (2020) 1564–1567.
[16] K. Sunada, M. Minoshima, K. Hashimoto, Highly efficient antiviral and antibacterial activities of solid-state cuprous compounds, J. Hazard. Mater. 235-236 (2012) 265–270.
[17] G. Borkow, H.H. Lara, C.Y. Covington, A. Nyamathi, J. Gabbay, Deactivation of human immunodeficiency virus type 1 in medium by copper oxide-containing filters, AAC 52 (2) (2008) 518–525.
[18] S. Behzadinasab, A. Chin, M. Hosseini, L. Poon, W.A. Ducker, A surface coating that rapidly inactivates SARS-CoV-2, ACS Appl. Mater. Interfaces 12 (31) (2020) 34723–34727.
[19] S.L. Warnes, Z.R. Little, C.W. Keevil, R. Colwell, Human coronavirus 229E remains infectious on common touch surface materials, mBio 6 (6) (2015), https://doi.org/10.1128/mBio.01697-15.
[20] M. Pourbaix, Atlas of Electrochemical Equilibria in Aqueous Solutions, National Association of Corrosion Engineers, Houston, Tex., 1974.